Energies **2014**, *7*, 6856-6885; doi:10.3390/en7116856

OPEN ACCESS

energies

ISSN 1996-1073

www.mdpi.com/journal/energies

Article

Simplified Analysis of the Electric Power Losses for On-Shore Wind Farms Considering Weibull Distribution Parameters

Antonio Colmenar-Santos [1,*], Severo Campíñez-Romero [1], Lorenzo Alfredo Enríquez-Garcia [2] and Clara Pérez-Molina [1]

[1] Industrial Engineering Higher Technical School, Spanish University for Distance Education, Juan del Rosal St., 12, Madrid 28040, Spain; E-Mails: scampinez1@alumno.uned.es (S.C.-R.); clarapm@ieec.uned.es (C.P.-M.)

[2] Escuela Superior Politécnica de Chimborazo, Riobamba-Chimborazo, EC060103, Ecuador; E-Mail: lorenzenriquez@yahoo.com

* Author to whom correspondence should be addressed; E-Mail: acolmenar@ieec.uned.es; Tel.: +34-913-987-788; Fax: +34-913-986-028.

External Editor: Frede Blaabjerg

Received: 14 July 2014; in revised form: 20 August 2014 / Accepted: 17 October 2014 / Published: 28 October 2014

Abstract: Electric power losses are constantly present during the service life of wind farms and must be considered in the calculation of the income arising from selling the produced electricity. It is typical to estimate the electrical losses in the design stage as those occurring when the wind farm operates at rated power, nevertheless, it is necessary to determine a method for checking if the actual losses meet the design requirements during the operation period. In this paper, we prove that the electric losses at rated power should not be considered as a reference level and a simple methodology will be developed to analyse and foresee the actual losses in a set period as a function of the wind resource in such period, defined according to the Weibull distribution, and the characteristics of the wind farm electrical infrastructure. This methodology facilitates a simple way, to determine in the design phase and to check during operation, the actual electricity losses.

Keywords: wind farm; electric losses; Weibull distribution

---

1. Introduction

Electric losses do not have an important effect on the net electricity production of a wind farm (WF), but due to the fact that they are constantly present for the entire service life of the WF, it is necessary to implement technical measures to limit them. Nevertheless, yearly losses around 2%–3% of the energy generated occur [1,2].

Usually the electric losses in onshore and offshore WFs are calculated from the estimated yearly capacity factor (The capacity factor, CF is defined, in a yearly period, as the percentage of the year during which the WF should have been working at nominal power to generate the entire production obtained in the year. The gross value, Gross CF, does not include the wake losses, the electric losses up to the point where the electricity fed into the grid is measured, and the production losses due to the mechanical availability of the WTG. The net value, Net CF, includes the effect of all the aforementioned losses expressed as a percentage) corresponding with long-term wind conditions [3,4] and the rated power of the WF [5–7]. These estimated electric losses at rated power are used in the design of the WF for setting technical requirements and to determine the foreseen net generation. The use of this method, considering the non-linear dependency of the electric losses with respect to the power flow, as well as the influence of the WF topology and the distribution of the wind in the set period, can introduce an important error in the business plan if the estimate of the losses at rated power is used as a reference to reduce the generation in the WF and the associated incomes for selling the net electricity fed into the system [6,8], principally because the error in such estimates will affect the cash flows during the whole service life of the WF.

Lately, feed-in-tariffs have been drastically reduced [9,10], the prices in power purchase agreements have been decreasing [11–13] and some competitive mechanisms have been included by public administrations in the processes for awarding WF licenses [14,15], so it is necessary to take to the extreme measures to improve the efficiency as well as implement systems and procedures to confirm the operation under the right conditions. For all of these reasons, the WF owners and their technical advisors include in the request for construction proposals and the subsequent contracts, the definition of methods to check if the electric infrastructures are working properly and producing losses in the guaranteed range. Once again it is practically unfeasible trying to compare the actual measured value with the one used in the design when its calculation is based in the CF and the operation at rated power [6].

The issue, although easy to deal with from a technical point of view, presents a friction point between the owner, the contractor, as designer of the WF, and the operator, perhaps due to the fact that the analysis and the subsequent result is not quite intuitive because the more energy is produced by the WF, the less electrical losses result, as a percentage, and in any case they are always different from those obtained with the classical method of calculation based in the operation at rated power. The study can be done with power flow analysis software, but this approach needs the creation of a complex model of the WF and the wind resource for every WTG and every set period.

The aim of this article is to develop a simple methodology to determine a range for the foreseen electric losses and to confirm, at any time, if the actual losses are in the right range and, therefore, if the WF is working properly. The methodology takes into account the characteristics of the wind resource, modelled according to a standard probability function in the wind sector: the Weibull distribution [16,17]. The method also is intended to be a practical tool for the owner, to put a cap on the reduction in the

incomes result of the electrical losses and, together with the constructor and the operator of the WF, to establish requirements for design and construction and to implement appropriate working tests. In brief, the method has a practical approach, and it is focused on helping to the definition and later confirmation of the electricity losses.

The approach to define the wind resource in order to be used in the losses calculation is presented in Section 2. In Section 3, two methods for calculating the electric losses are given, as well as the results for its application in a WTG, in a cluster or circuit of WTGs and in the entire WF. The financial impact in the cash flows and the net value of the WF is shown in Section 4, and finally, the conclusions are presented in Section 5.

2. Characterization and Variability of the Wind Resource

The Weibull distribution is the most suitable probability function to represent the wind resource in a specific site along a specific period of time [16,17]. The equation for the density function is [18,19]:

$$f(s) = \frac{k}{\lambda}\left(\frac{s}{\lambda}\right)^{k-1} e^{-\left(\frac{s}{\lambda}\right)^{k}} \quad (1)$$

where k and λ, are, respectively, the shape and scale parameters, and together define the wind resource. The variable s represents the wind speed. Nevertheless, the wind resource at a given site is variable with time and the period considered and so, the Weibull distribution parameters vary as well even though this period represents the same time (*i.e.*, a specific month in the year).

With the aim to illustrate this wind resource variability, actual data from a meteorological station equipped with anemometers and wind vanes, both calibrated, located at a height of 80 m on the west coast of the Republic of South Africa have been used (nowadays there is an ongoing process of request for proposals for the construction, operation and maintenance of a WF at the selected location; the exact location is not given because this information is under a non-disclosure agreement with the owner of the data). Figure 1 shows the graphic representation of the Weibull density function for the real wind resource in the year 2012 and within each one of the months of 2012 and the Table 1 presents the variation of the Weibull parameters and the mean wind speed in the same periods.

Figure 1. Weibull distribution functions corresponding with the year 2012.

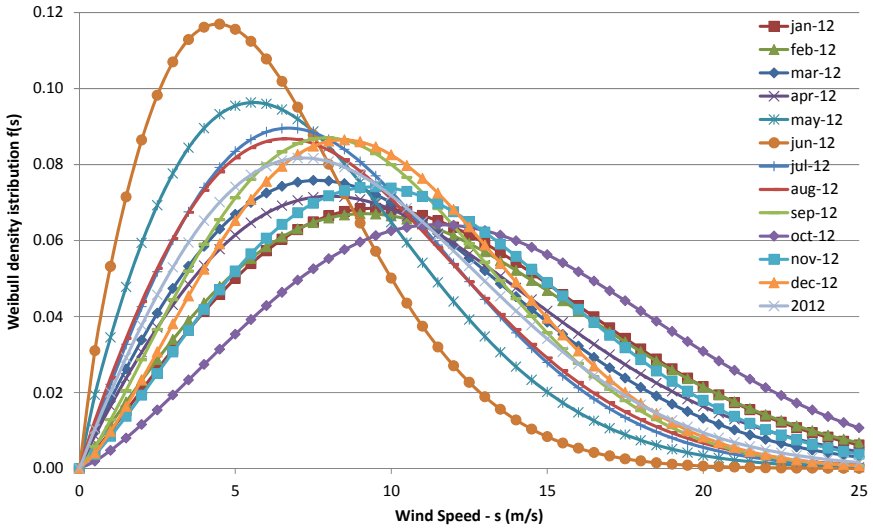

Table 1. Variation of the Weibull parameters and the mean wind speed in 2012.

Weibull parameters	Period												
	Jan.	**Feb.**	**Mar.**	**Apr.**	**May**	**Jun.**	**Jul.**	**Aug.**	**Sep.**	**Oct.**	**Nov.**	**Dec.**	**Year**
Shape—k	2.09	2.02	1.94	1.93	1.85	1.81	1.99	1.93	2.19	2.30	2.21	2.28	1.96
Scale—λ (m/s)	12.92	12.86	11.09	11.72	8.50	6.90	9.54	9.67	10.48	14.73	12.40	10.89	10.35
Mean wind speed	11.44	11.39	9.83	10.39	7.54	6.14	8.45	8.57	9.28	13.05	10.98	9.64	9.17

Figure 2 shows the power density (wind power density is defined in a specific period of time as the mean power available per square meter of swept area of a wind turbine) for the wind conditions included in Table 1. As it may be noticed, the energetic content of the wind resource is not constant, and hence, due to the fact that the electricity losses in the WF depend on the power generated by every WTG, it is essential to analyse the electrical losses in a specific period of time, in which the wind resource will be modelled with the corresponding Weibull parameters, in general different in every period.

Figure 2. Wind power density in 2012.

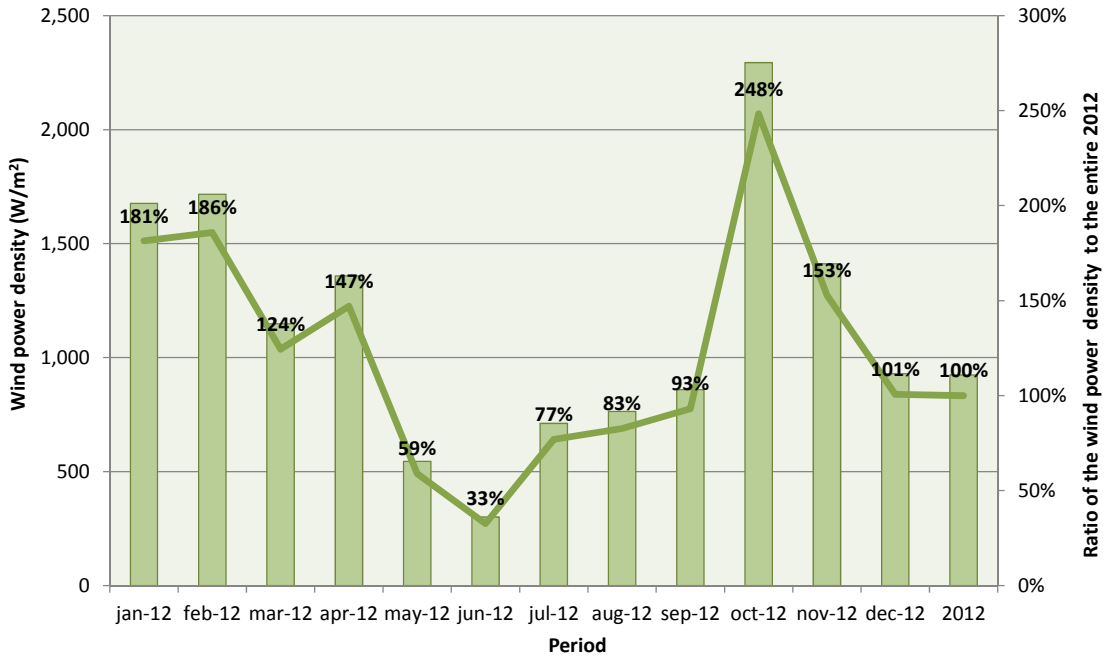

3. Calculation of the Electrical Losses

In general, the WF, including the systems to connect it to the electric grid, implies a simple electrical circuit to be solved with the traditional tools of power flow analysis, but even so, a reduced number of WTGs gives a high number of buses (every WTG adds two buses and four equations to the problem: the connection of the generator to the step-up transformer and the connection of the latter to the collector system) and the analysis requires the use of expert software and therefore to make a model for the entire WF including all the electrical infrastructures.

Most of the WTGs include systems to allow the regulation of the voltage in the PCC by means of controlling the reactive power interchanged with the grid [20]. Thanks to this capacity, the WFs contribute actively to keep the voltage levels within the targets set up by the grid operators independently of the flows of active power. Under normal conditions of operation, the flows of reactive power are small

(the power factor is close to one) and the voltage magnitudes in the buses of the WF are very close to the nominal value. In this article, we study the active power losses, and hence, considering the aforementioned statements, a simplification in the calculation can be implemented with the application of the flow analysis in direct current to the study of the active power flows. This simplification implies a certain error that will not affect the comparison between the traditional method to calculate the electric losses and the methodology introduced in this article (to check the validity of the assumptions made to use the power flow analysis in direct current the WF studied was simulated running for several wind conditions the classical power flow analysis in alternating current, in all the simulations the results validated the assumptions, giving minimal differences less than 6° between the angles in adjacent buses and less than the 1.35% respect to the nominal value in the voltage magnitude).

Therefore, all the cases analysed in this article have been carried out by means of the application of the analysis of power flow in direct current according to the basics indicated in [21].

3.1. Application to One WTG

The Figure 3 shows the single line diagram of a WTG connected to the electric grid in the BUS_{PCC}.

Figure 3. Single line diagram of one WTG.

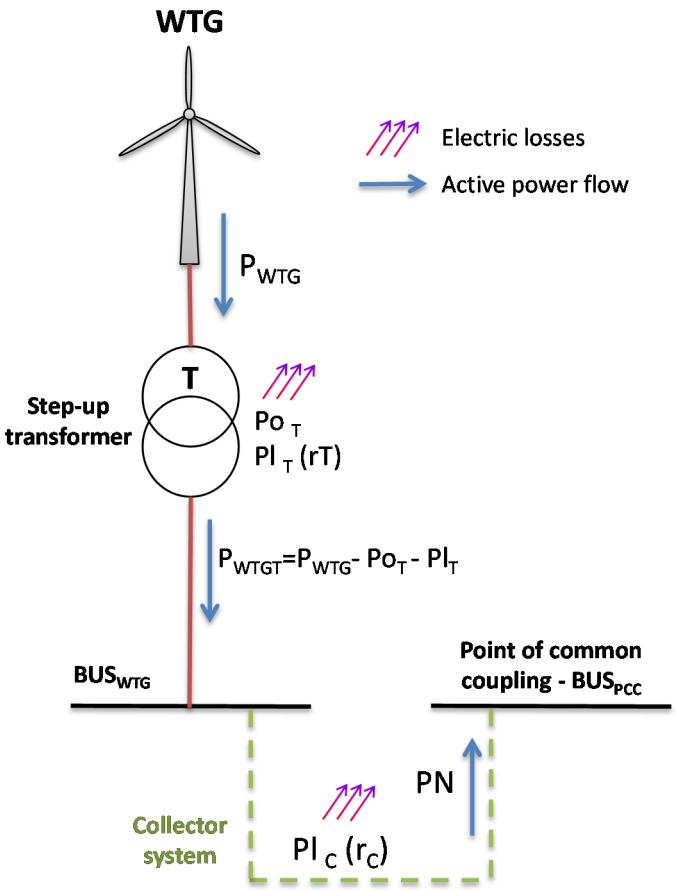

The active power injected in the BUS_{WTG} is the active power generated by the WTG reduced by the power losses in the step-up transformer, both load and no-load. This power is designated as P_{WTGT} (all the powers are dependent on the instantaneous speed of the wind at the hub elevation, so they should be represented with g(s)-type functions, to simplify the equations, the reference to the wind dependence

has not been included except in those cases in which it has been considered necessary to understand the right meaning. Hence in the rest of the article $P_{ANY}(s) = P_{ANY}$), and its formula is:

$$P_{WTGT} = P_{WTG} - (Po_T + Pl_T) \tag{2}$$

The no-load power losses Po_T will be constant while the voltage remains constant, a premise for using the power flow analysis in direct current. The load losses in the step-up transformer Pl_T will depend on the power flow, therefore, these will be calculated as follows:

$$Pl_T = \left(\frac{P_{WTG} - Po_T}{V_{GRID}}\right)^2 r_T = (P_{WTG} - Po_T)^2 \frac{r_T}{{V_{GRID}}^2} \tag{3}$$

In the cable that connects the BUS_{WTG} to the BUS_{PCC}, there will be an active power losses Pl_C. The active power injected in the BUS_{PCC}:

$$PN = [P_{WTG} - (Po_T + Pl_T)] - Pl_C \tag{4}$$

$$PN = P_{WTG} - Po_T - (P_{WTG} - Po_T)^2 \frac{r_T}{{V_{GRID}}^2} - Pl_C \tag{5}$$

According to [21] the electric losses in the collector system cable are:

$$Pl_C = \left[P_{WTG} - Po_T - (P_{WTG} - Po_T)^2 \frac{r_T}{{V_{GRID}}^2}\right]^2 \frac{r_C}{{V_{GRID}}^2} \tag{6}$$

The expression for the active power injected in the BUS_{PCC} can be:

$$\begin{aligned} PN = {} & P_{WTG} - Po_T - (P_{WTG} - Po_T)^2 \frac{r_T}{{V_{GRID}}^2} \\ & - \left[P_{WTG} - Po_T - (P_{WTG} - Po_T)^2 \frac{r_T}{{V_{GRID}}^2}\right]^2 \frac{r_C}{{V_{GRID}}^2} \end{aligned} \tag{7}$$

Defining P_{WTGT} as the power generated by the group WTG reduced by the losses in the step-up transformer as:

$$P_{WTGT} = P_{WTG} - Po_T - (P_{WTG} - Po_T)^2 \frac{r_T}{{V_{GRID}}^2} \tag{8}$$

The net power delivered to the coupling point is:

$$PN = P_{WTGT} - P_{WTGT}^2 \frac{r_C}{{V_{GRID}}^2} \tag{9}$$

Therefore, the total losses will be:

$$Pl = P_{WTG} - \left(P_{WTGT} - P_{WTGT}^2 \frac{r_C}{{V_{GRID}}^2}\right) \tag{10}$$

The losses at rated power can be calculated with the following expression:

$$El_{FP} = \frac{Pl_{rated}}{P_{rated}} \tag{11}$$

3.1.1. Energy Losses

Once calculated the total losses Pl, the energy lost in the set period T is:

$$El = \int_0^T Pl(t)\,dt = T\int_0^\infty Pl(s)\,f(s)\,ds \tag{12}$$

where $f(s)$ is the Weibull density function shown in Equation (1) and $Pl(s)$ is the function that links the electric losses with the instantaneous wind speed at WTG hub elevation. As shown in Figure 4, the WTG power curve can be divided in four sections, in which is possible to formulate an analytical expression linking the wind speed at hub height and the power generated and therefore with the electric losses.

Figure 4. WTG power curve with and without the internal transformer. Both divided into sections.

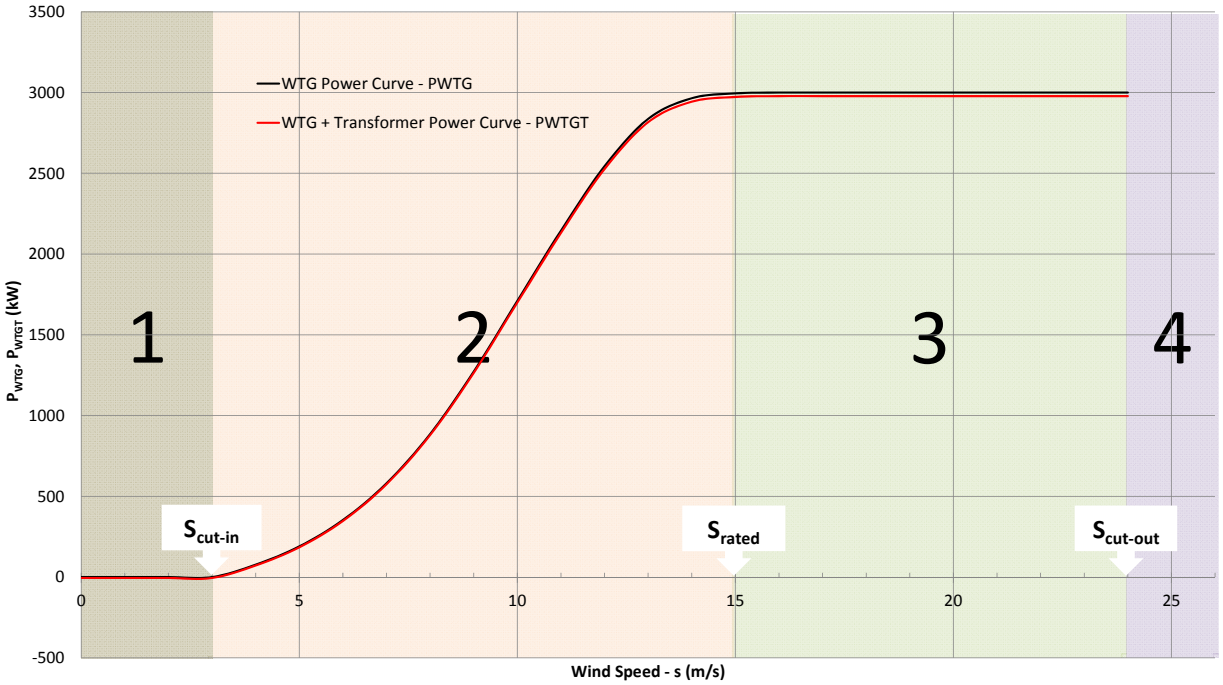

In Section 1, $s \in [0, s_{cut-in}]$ and 4, $s \in [s_{cut-in}, \infty]$, the power generated by the WTG is zero, therefore:

$$P_{WTG}^{(1} = P_{WTG}^{(4} = 0 \tag{13}$$

$$P_{WTGT}^{(1} = P_{WTGT}^{(4} = -Po_T - (-Po_T)^2 \frac{r_T}{{V_{GRID}}^2} \tag{14}$$

$$Pl^{(1} = Pl^{(4} = Pl_o = Po_T + (-Po_T)^2 \frac{r_T}{{V_{GRID}}^2} + \left[-Po_T - (-Po_T)^2 \frac{r_T}{{V_{GRID}}^2}\right]^2 \frac{r_C}{{V_{GRID}}^2} \tag{15}$$

In Section 3, $s \in [s_{rated}, s_{cut-out}]$, the WTG operates at rated power for all the wind speed range, then:

$$P_{WTG}^{(3} = P_{rated} \tag{16}$$

$$P_{WTGT}^{(3} = P_{rated} - Po_T - (P_{rated} - Po_T)^2 \frac{r_T}{{V_{GRID}}^2} \tag{17}$$

$$Pl^{(3} = Pl_{rated} = Po_T + (P_{rated} - Po_T)^2 \frac{r_T}{{V_{GRID}}^2} + \left[P_{rated} - Po_T - (P_{rated} - Po_T)^2 \frac{r_T}{{V_{GRID}}^2}\right]^2 \frac{r_C}{{V_{GRID}}^2} \tag{18}$$

In Section 2, $s \in [s_{cut-in}, s_{rated}]$, the power curve can be modelled using a polynomial expression [22–24] as given below (the fitting of $P_{WTG}^{(2}$, $P_{WTGT}^{(2}$ and $(P_{WTGT}^2)^{(2}$ with fourth degree polynomials, considering the power curve shown in Figure 4, gives coefficients of correlation R^2 above 0.99):

$$P_{WTG}^{(2} = \sum_{m=1}^{4} a_m s^m \tag{19}$$

$$P_{WTGT}^{(2} = \sum_{n=1}^{4} b_n s^n \tag{20}$$

$$(P_{WTGT}^2)^{(2} = \sum_{p=1}^{4} c_p s^p \tag{21}$$

$$Pl^{(2} = \sum_{m=1}^{4} a_m s^m - \left(\sum_{n=1}^{4} b_n s^n - \frac{r_C}{{V_{GRID}}^2} \sum_{p=1}^{4} c_p s^p\right) \tag{22}$$

Considering these polynomial expressions, the Equation (12) can be re-written as follows:

$$\frac{El}{T} = \int_0^{s_{cut-in}} Pl^{(1}(s)\, f(s) ds + \int_{s_{cut-in}}^{s_{rated}} Pl^{(2}(s)\, f(s) ds + \int_{s_{rated}}^{s_{cut-out}} Pl^{(3}(s)\, f(s) ds + \int_{s_{cut-out}}^{\infty} Pl^{(4}(s)\, f(s) ds \tag{23}$$

Because the losses in Sections 1, 3 and 4 are constant, and taking into account the relation between the Weibull density function $f(s)$ and the distribution function $F(s)$:

$$\int_{s_1}^{s_2} f(s)\, ds = F(s_2) - F(s_1) \tag{24}$$

where $F(s)$, for a Weibull distribution has the following expression:

$$F(s) = 1 - e^{-\left(\frac{s}{\lambda}\right)^k} \tag{25}$$

$$\frac{El}{T} = Pl_o\, F(s_{cut-in}) + \int_{s_{cut-in}}^{s_{rated}} Pl^{(2}(s)\, f(s) ds + Pl_{rated}\, [F(s_{cut-out}) - F(s_{rated})] + Pl_o\, [1 - F(s_{cut-out})] \tag{26}$$

$$Pl^{(2} = \sum_{m=1}^{4} a_m s^m - \left(\sum_{n=1}^{4} b_n s^n - \frac{r_C}{{V_{GRID}}^2} \sum_{p=1}^{4} c_p s^p\right) \tag{27}$$

$$\frac{El^{(2}}{T} = \int_{s_{cut-in}}^{s_{rated}} \left[\sum_{m=1}^{4} a_m s^m - \left(\sum_{n=1}^{4} b_n s^n - \frac{r_C}{{V_{GRID}}^2} \sum_{p=1}^{4} c_p s^p \right) \right] f(s) ds \quad (28)$$

Considering the Appendix A, the solution for this integral is:

$$\frac{El^{(2}}{T} = \sum_{m=1}^{4} \left(a_m - b_m + \frac{r_C}{{V_{GRID}}^2} c_m \right) \lambda^m \left\{ \gamma \left[\left(\frac{m}{k} + 1 \right), \left(\frac{s_{rated}}{\lambda} \right)^k \right] - \gamma \left[\left(\frac{m}{k} + 1 \right), \left(\frac{s_{cut-in}}{\lambda} \right)^k \right] \right\} \quad (29)$$

Therefore, the expression for the total energy losses in the set period T is:

$$\frac{El}{T} = Pl_o \left[1 + F(s_{cut-in}) - F(s_{cut-out}) \right] + \sum_{m=1}^{4} \left(a_m - b_m + \frac{r_C}{{V_{GRID}}^2} c_m \right) \lambda^{m-1} \left\{ \gamma \left[\left(\frac{m}{k} + 1 \right), \left(\frac{s_{rated}}{\lambda} \right)^k \right] - \gamma \left[\left(\frac{m}{k} + 1 \right), \left(\frac{s_{cut-in}}{\lambda} \right)^k \right] \right\} + Pl_{rated} \left[F(s_{cut-out}) - F(s_{rated}) \right] \quad (30)$$

3.1.2. Energy Generated

Considering again the division of the WTG power curve into four sections, the expression for the electricity generated is given by:

$$\frac{Eg}{T} = \int_0^{s_{cut-in}} {P_{WTG}}^{(1}(s) f(s) ds + \int_{s_{cut-in}}^{s_{rated}} {P_{WTG}}^{(2}(s) f(s) ds + \int_{s_{rated}}^{s_{cut-out}} {P_{WTG}}^{(3}(s) f(s) ds + \int_{s_{cut-out}}^{\infty} {P_{WTG}}^{(4}(s) f(s) ds \quad (31)$$

Taking into account the Expressions (13), (16) and (19), the electricity generated can be formulated as follows:

$$\frac{Eg}{T} = \int_{s_{cut-in}}^{s_{rated}} \left[\sum_{m=1}^{4} a_m s^m f(s) \right] ds + P_{rated} \left[F(s_{cut-out}) - F(s_{rated}) \right] \quad (32)$$

And according to the Appendix A, the final solution is:

$$\frac{Eg}{T} = \sum_{m=1}^{4} a_m \lambda^m \left\{ \gamma \left[\left(\frac{m}{k} + 1 \right), \left(\frac{s_{rated}}{\lambda} \right)^k \right] - \gamma \left[\left(\frac{m}{k} + 1 \right), \left(\frac{s_{cut-in}}{\lambda} \right)^k \right] \right\} + P_{rated} \left[F(s_{cut-out}) - F(s_{rated}) \right] \quad (33)$$

3.1.3. Characterization of the Electrical Infrastructures

For the analyses of the losses, the equipment was modelled with the following parameters and variables (the equivalent circuit is shown in Figure 5)

- The WTG as an ideal generator of which instantaneous power output is obtained from the power curve corresponding with the wind speed at the hub height. This representation does not introduce

error in the calculations because the power curve gives the net power output for all the wide range of operating voltage of the WTG.

- The WTG step-up transformer by means of a parallel resistance for the non-load losses Po_T and a serial resistance r_T for the load losses.
- The collector system cable between the BUS_{WTG} and the BUS_{PCC} with a serial resistance r_C.

Figure 5. Equivalent electric circuit for the simulation.

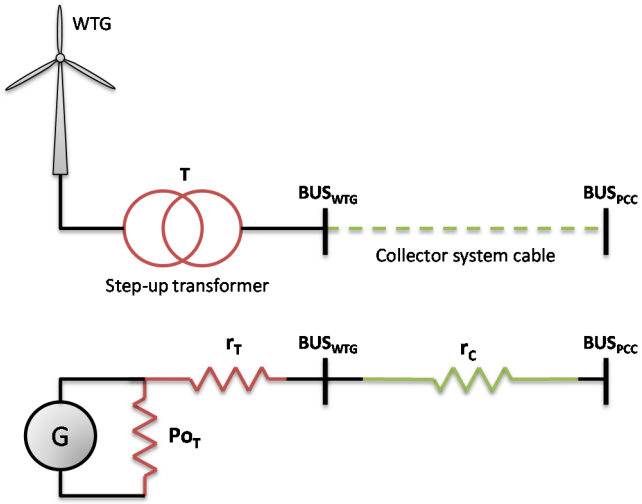

To run the simulations, representative values based on actual data from commercial equipment widely used in the construction of the WFs have been assigned to the variables of the equivalent circuit. Regarding the WTG, the one selected was the V112 of Vestas [25], with 3 MW of rated power and 112 m of rotor diameter. The power curve for this WTG is shown in Figure 4. The main characteristics are similar to those of the WTGs of other manufacturers (Siemens [26], Alstom [27], Gamesa [28], *etc.*). The values considered for the non-load and load losses of the step-up transformer correspond with standard transformer supplied by Vestas along with the WTG.

The connections of the WTGs to the collector system are usually done with isolated aluminium cables buried in trenches. The size of the cables is calculated according to the requirements of ampacity, short-circuit withstand and drop voltage. The main manufacturers offer sizes ranging between 10 mm^2 and 500 mm^2, but due to a matter of economy of scale, a maximum of two or three different sizes are usually used in the collector system. In the simulations, a mean size was supposed for the collector system. The insulation of the cable affects its electric resistance. Currently, three different technologies are predominant in the market: polyvinyl chloride (PVC); cross-linked polyethylene (XLPE) and ethylene propylene. The most used insulation materials are XLPE and EPR and in both cases the effect on the resistance presented by the cable are equal [29].

Respect to the length of the collector system, it will be directly conditioned by the WTG layout. Obviously, the best positions should be selected in terms of wind resource. With the objective of maximizing the generation at a minimum cost, several methods have been suggested to optimize WF layouts [30–33]. However, very often, especially at sites where the wind resource is homogenous over all the area available and for the purpose of minimising losses caused by the wake effect [31,34,35] the WTGs are located within a distance in the range of two or three times the length of the WTG rotor diameter in the

line perpendicular to the prevailing wind direction [18,36]. In our case, according to these basic rules, the distance should be between 224 m and 366 m, therefore a mean length of 350 was selected.

To define the voltage magnitude of the collector system, it is important to consider on the one hand that the size of the switchgears and the step-up transformers increase with the magnitude and that these elements are usually installed inside the WTGs with space limitations. On the other hand, using a low voltage level implies higher currents in the collector system and the use of bigger sizes in the cables. The market offer nowadays equipment with nominal voltages values up to 40 kV [37–39] therefore a typical standard voltage level of 36 kV was selected.

A summary with of characteristics of the infrastructure elements used in the simulations is included in Table 2.

Table 2. Characteristics of the infrastructure elements used in the simulation of a WTG.

Element	**Name**	**Value**	**Unit**	**Comment**
WTG	Manufacturer and type	Vestas V112-3 MW	–	Class I WTG [40] 112 m of rotor diameter
	Power curve	Figure 4	–	Vestas standard
Step-up transformer	Manufacturer and type	Standard for V112-3 MW	–	–
	Po_T	5.3	kW	Manufacturer data for the WTG selected
	r_T	2.42	Ω	Manufacturer data for the WTG selected. Corresponds with a 0.7% of positive sequence short-circuit resistance at the transformer rated power
Collector system	V_{GRID}	36	kV	Typical
Interconnection cable to the collector system	Length (L)	350	m	The selected WTG has a 112 m rotor diameter. To reduce weak losses the separation between neighbour WTGs should be in the range of 2 or 3 times the length of the rotor diameter
	Material	Al		Typical
	Size	120	mm^2	Medium value
	Insulation material	XLPE/EPR		Typical
	r_C per km	0.3226	Ω/km	–
	r_C	0.1129	Ω	–

3.1.4. Calculation and Simulation Results

The expression for the relative energy losses is:

$$El(\%) = \frac{El}{Eg} \times 100 \quad (34)$$

The calculation of the electricity generation and losses for a wide range of values of the Weibull parameters was done using MATLAB [41] The behaviour of the WTG and the associated electric infrastructures detailed in the Table 2 was simulated to calculate the electricity generation by applying Equation (30) and the electricity losses by applying Equations (33) and (34). The results, illustrated in Figure 6, show that, in relation with the losses calculated when the WTG operates at rated power and for any wind regime considered, the actual electric losses are always higher, reaching even the double.

Figure 6. Electric losses of the energy generated for a WTG as a function of the Weibull parameters representatives of the period considered.

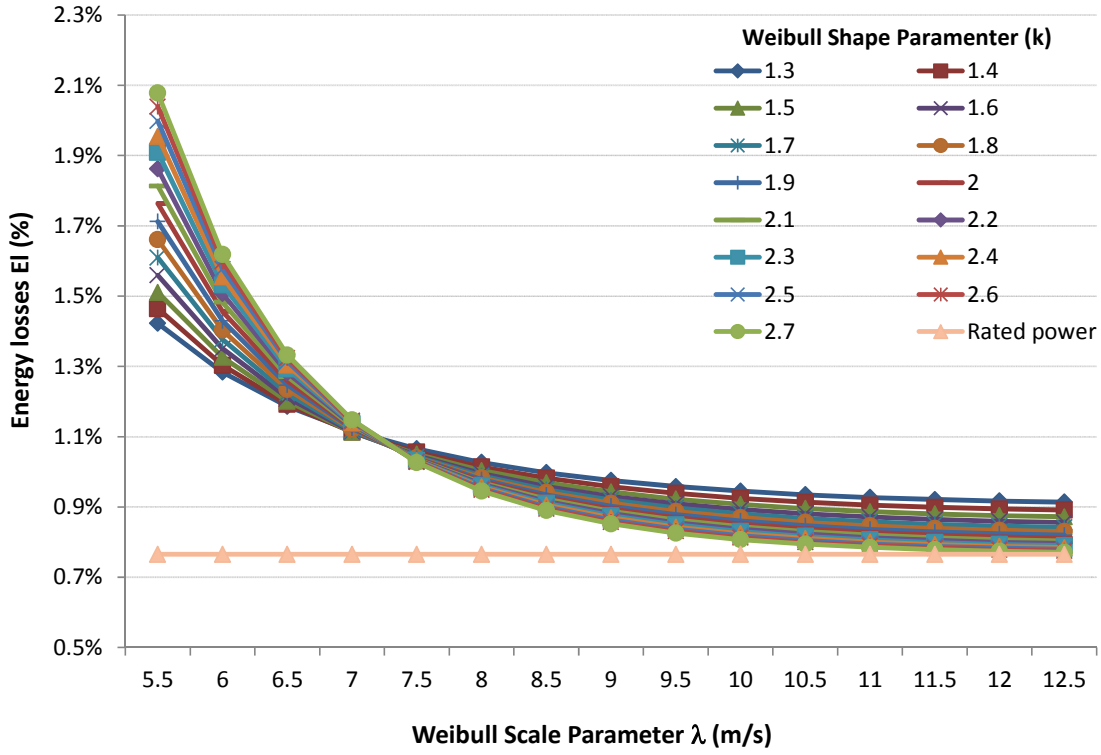

3.2. Application to a WF

Generally, WFs are made up of several WTGs. In the design stage, the WTGs are grouped in evacuation circuits under criteria for making best use of the capacity of the equipment and for optimizing the total cost of the cable needed to form the collector system.

The number of WTGs for every single circuit depends on several factors: the relative location of the WTG among themselves and in relation to the substation; the WTG rated power; the collector system voltage magnitude and the capacity of the switchgears because the total current of the circuit flow through the last WTG. Typically, the switchgears supplied with the WTGs have a rated current of 630 A [37–39], thus for a WTG rated power of 3 MW, a nominal voltage of 36 kV in the collector system and a minimum load factor of 0.8, the maximum number of WTGs per circuit should be:

$$n_i < \frac{630\ A}{\frac{0.8 \times 3{,}000\ \text{kW}}{\sqrt{3} \times 36\ \text{kV}}} \sim 10\ \text{WTGs} \tag{35}$$

Nevertheless, taking into account reliability criteria, it is very common to do the design in groups of less WTGs per circuit, with the criterion of facilitating the operation of the WF and minimizing the losses of generation in case of trip or failure of the switchgear that connects the circuit to the substation. However, it is not reasonable to have a small number of WTGs per circuit, because it would imply a high number of circuits and an increase of the length of the collector system cables and the number of switchgears in the substation. An optimization, taking into account the aforementioned factors, gives a typical number of 3 circuits with 5 or 6 WTGs per circuit for a WF around 50 MW [7,42,43].

Figure 7 shows the single line diagram of a 6 WTG circuit as well as the electric infrastructure to connect it to the PCC.

Figure 7. Single line diagram of a circuit and the power evacuation infrastructure up to the PCC.

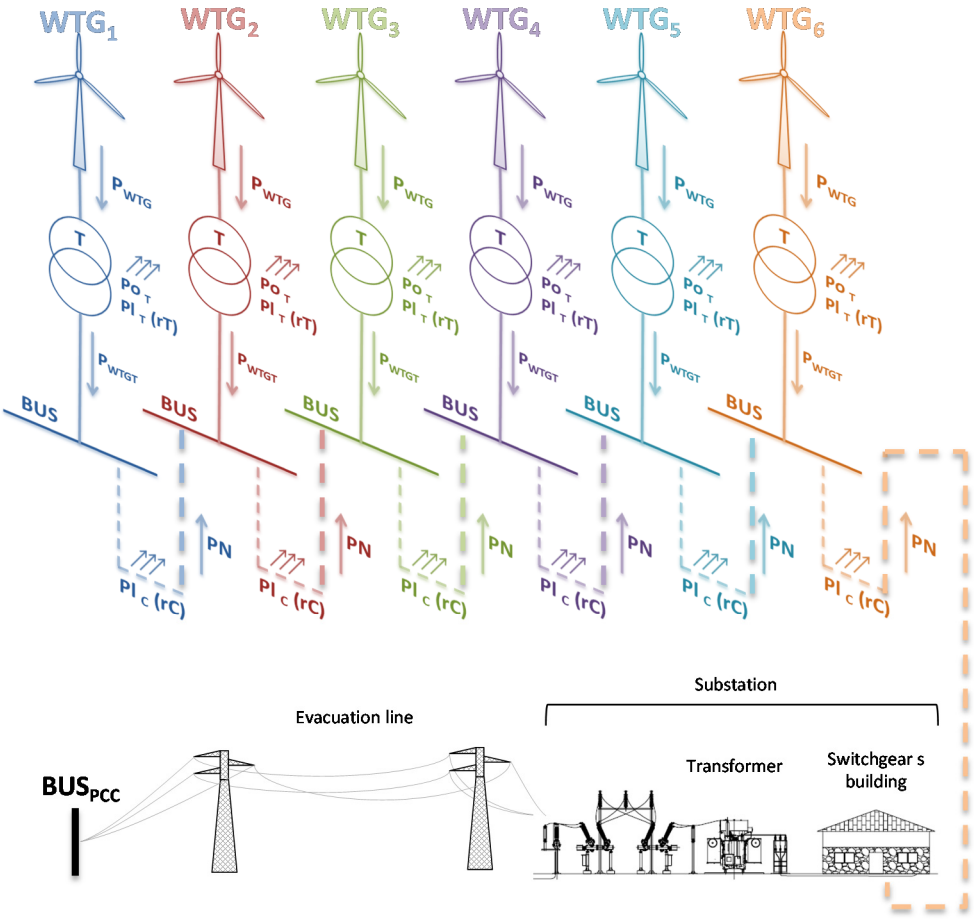

3.2.1. Energy Losses

In the general case, which single line diagram and electric equivalent circuit are shown in Figure 8, the active power injected in a generic bus named $i + 1$ coming from the previous bus i through the collector system cable is the result of:

1. The active power generated by the WTG, P_{WTGi}, reduced by the losses of the step-up transformer $(Po_{Ti} + Pl_{Ti})$.
2. The addition of the net active power coming from the previous bus, PN_{i-1}.
3. The subtraction of the electric losses in the cable between both cables, Pl_{Ci}.

Figure 8. WF single line and electric equivalent diagrams.

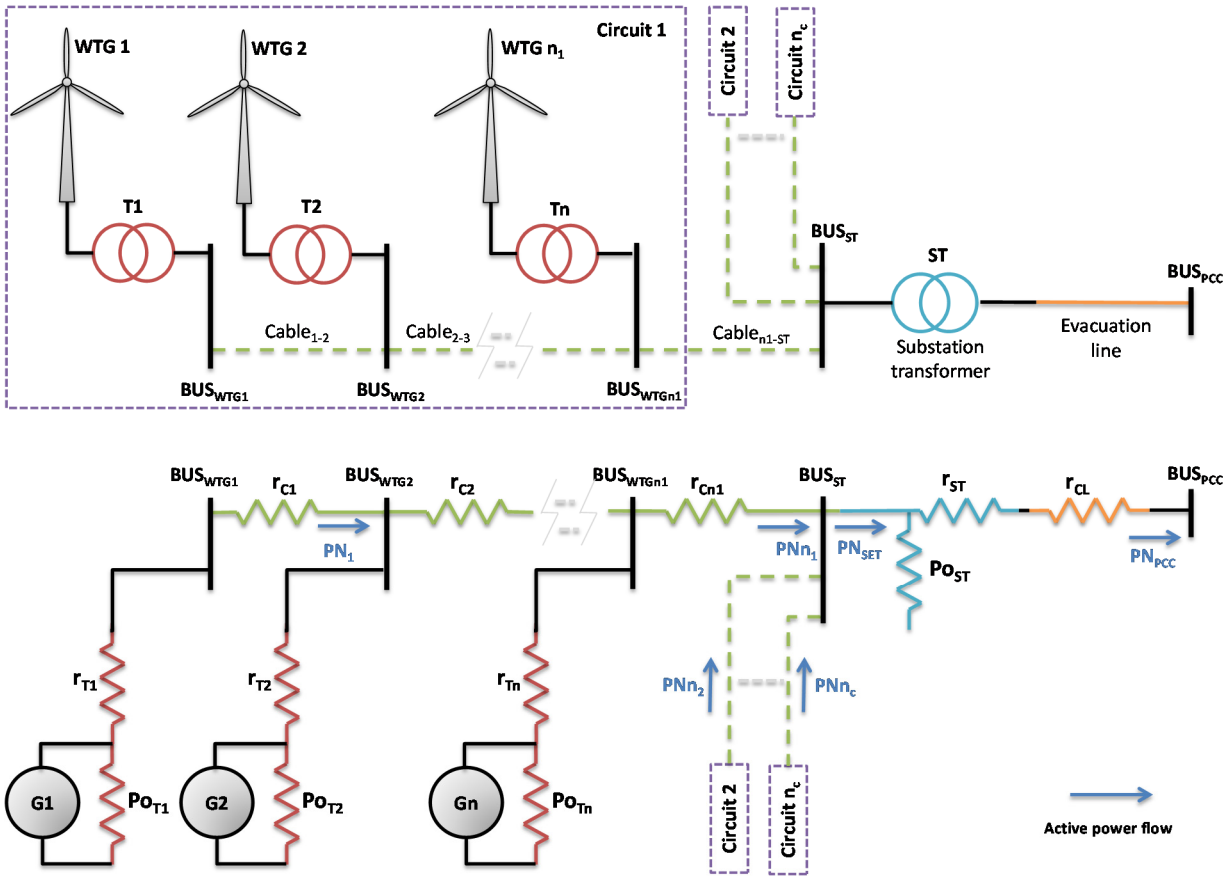

Considering Equations (3) and (6), corresponding to the losses in the step-up transformer and in the collector system cable, the expression for the net power injected in the BUSST is:

$$PN_i = PN_{i-1} + P_{WTGi} - Po_{Ti} - (P_{WTGi} - Po_{Ti})^2 \frac{r_{Ti}}{V_{GRID}{}^2} - \left[PN_{i-1} + P_{WTGi} - Po_{Ti} - (P_{WTGi} - Po_{Ti})^2 \frac{r_{Ti}}{V_{GRID}{}^2}\right]^2 \frac{r_{Ci}}{V_{GRID}{}^2} \quad (36)$$

In general, the wind of each WTG hub will be different, but it does not present important differences that affect qualitatively the objectives of the simulation. In fact, the effect would be similar to supposing a different scale parameter for the Weibull representation of the wind resource for each turbine. As can be seen in Figure 6, for a WTG a variation of 5% in the scale parameter representative of the period considered in the calculations has a limited impact in the losses exceeding 10% only for very low resource periods. This assumption is applicable except in special conditions depending on the complexity of the land orography, the layout of the WTG and the wind direction. In those cases different Weibull functions should be considered. Therefore, in the calculations it was supposed that the wind in every single WTG hub is the same and accordingly to the power generated is also the same and equal to P_{WTG}.

Likewise, the step-up transformers installed in each WTG will have the same characteristics, so that the no-load losses as well as the short-circuit resistance can be supposed the same for all of them.

Considering the aforementioned, for each one of the n_C circuits forming the WF, the net active power injected in the BUSST would be the result of Equation (36) particularized for the last WTG, so that, for a generic circuit *j*:

$$PN_{n_j} = PN_{n_{j-1}} + P_{WTG} - Po_T - (P_{WTG} - Po_T)^2 \frac{r_T}{{V_{GRID}}^2} - \left[PN_{n_{j-1}} + P_{WTG} - Po_T - (P_{WTG} - Po_T)^2 \frac{r_T}{{V_{GRID}}^2}\right]^2 \frac{r_{Ci}}{{V_{GRID}}^2} \quad (37)$$

The total net active power injected in the BUS_{ST} is the sum of the net power coming from all the circuits, so that:

$$PN_{SET} = \sum_{j=1}^{c} PN_{nj} \quad (38)$$

Finally, the active power delivered in the BUS_{PCC}, results reducing PN_{SET} by the step-up transformer losses (no-load and load) and the power losses in the evacuation line:

$$PN_{PCC} = PN_{SET} + (PN_{SET} - Po_{ST})^2 \frac{r_{ST}}{{V_{PCC}}^2} + \left[PN_{SET} - Po_{ST} - (PN_{SET} - Po_{ST})^2 \frac{r_{ST}}{{V_{PCC}}^2}\right]^2 \frac{r_{CL}}{{V_{PCC}}^2} \quad (39)$$

Taking into account that the number of WTGs in the WF is n_{WF}, the total active power generated is given by:

$$PG_{WF} = n_{WF}\, P_{WTG} \quad (40)$$

And therefore, the total active power losses in the WF are:

$$Pl_{\mathrm{WF}} = PG_{\mathrm{WF}} - PN_{PCC} \quad (41)$$

The electricity lost in the set period *T* is the result of the integration of the previous Equation (41) in such a period:

$$El_{WF} = \int_0^T Pl_{WF}(t)\, dt = T \int_0^{\infty} Pl_{WF}(s)\, f(s) ds \quad (42)$$

But now, the Equation (41) for $Pl_{WF}(s)$ does not allow a direct integration to obtain an analytic equation as it was done for a sole WTG. The fact that the losses in every part of the collector system depend recursively on the previous losses, and the simplification implemented by means of the substitution of the WTG power curve by a polynomial fitting, turn unmanageable the defined integral Equation (42).

In this case, instead of an analytical solution, the integral was solved in a discrete way. The Weibull wind distribution can be indicated in discrete intervals of the wind speed. In addition, WTG manufacturers give usually the power curve in a tabulated serial values relating the intervals of the wind speed at hub height with the power output. This way introduces a certain error dependent on the width of the interval, such that the wider the interval is, the higher the error is. At the limit, so that the interval was equal to zero, the solution would correspond with the analytical solution and the error would be zero. Anyway, considering the usual intervals given by manufacturers, 0.5 or 1 m/s, the error is not very relevant for the qualitative results of the simulations, due to the fact that both curves, power output and wind distribution, present smooth outlines and slopes, and therefore there will not be important variations in each interval (in order to delimit the margin error, a comparison between the results obtained with

Equation (30) and the discrete method developed in this section applied for one WTG was carried out, the differences were, for all the range of the Weibull parameters, lower than 4%).

From these discrete values for the wind resource and the power generated by each WTG it is possible to calculate for every single interval of the wind speed, the losses in all the collector system sections, all the circuits and finally the total losses for the entire WF. An example of the result obtained in the application of this method is shown in Figure 9, where the histograms for a wind resource with Weibull parameters k = 1.9 and λ = 10 m/s and a WF made up of three circuits with six WTGs in each one of the circuits (total WF power 3 × 6 × 3 = 54 MW) are illustrated.

Figure 9. Histograms for the wind density distribution and the power losses.

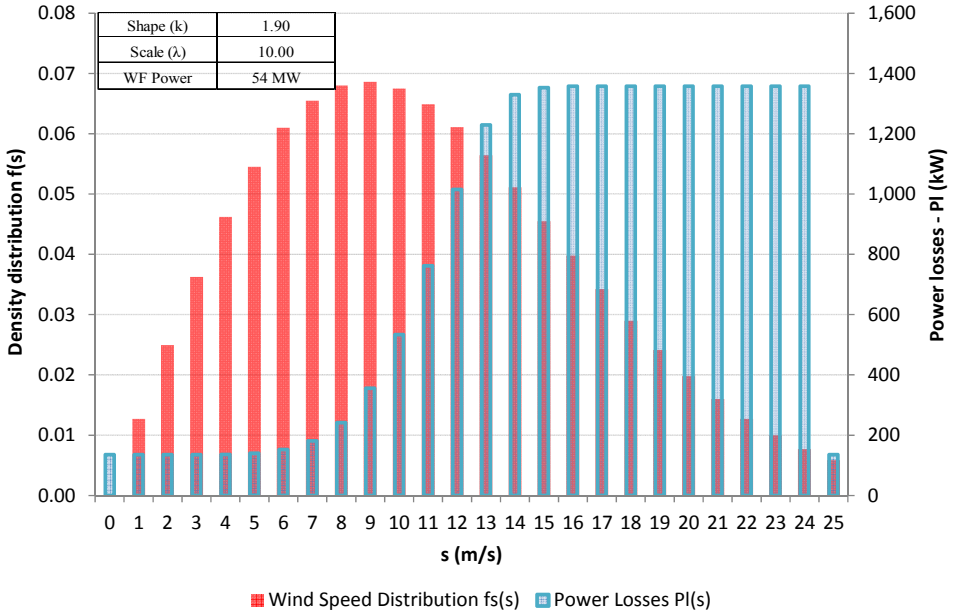

Finally, once the value of losses in each interval is obtained, the total electricity lost in the set period T, is given by:

$$El_{WF} = T \sum_{s=0}^{s_{cut-out}} Pl_{WF}(s)\, f(s) \Delta s \tag{43}$$

3.2.2. Energy Generated

Considering that the number of WTGs in the WF is n_{WF}, the total electricity generated by the WF is given by:

$$Eg_{WF} = n_{WF} \times Eg \tag{44}$$

where E_g is the electricity generated by every WTG calculated in Equation (33).

3.2.3. Characterization of the WF and the Electric Infrastructures

For the simulation of the WF, it is necessary to extend the modelling of the equipment developed in the Section 3.1.3., to the elements that connect the WTGs to the PCC: the substation transformer and the

evacuation line. The equivalent electric circuit is drawn in Figure 8. In the simulations these elements were represented by the following parameters:

- The substation transformer by means of a parallel resistance for the non-load losses Po_{ST} and a serial resistance r_{ST} for the load losses. Both parameters are obtained from the standard short-circuit and losses test carried out for every single transformer.
- The evacuation line between the substation (BUS_{ST}) and the BUS_{PCC} with a serial resistance r_C.
- The evacuation voltage magnitude is, in general, different and higher than the collector system voltage magnitude.

In the same way as the case of a sole WTG, to run the simulations, representative values based on actual data from commercial equipment widely used in the construction of the WFs [44–46] have been assigned to the variables of the equivalent circuit. The installed power of the WF was assumed to be a medium value of 54 MW, corresponding to 18 WTGs of 3 MW, distributed in three circuits with six WTGs each one. The PCC voltage magnitude was initially set in 132 kV, valid to evacuate the power capacity of the WF, and lately, as shown in Section 3.2.4., a sensitivity analysis respect to the voltage magnitude was carried out.

To define the parameters of the evacuation line, three different sizes of aluminium conductor steel reinforced (ACSR) were considered. This type of cable is very widely used for a wide range of power capacity and voltage magnitudes values [47,48]. First the simulation was made for a size of the conductor in accordance with the rest of the assumptions (WF power installed and voltage magnitude of the PCC) and then a sensitivity analysis respect to the variation of the size of the cable was carried out. The power transmission limits and the value of the resistance are shown in Table 3.

Table 3. Power transmission limits and resistance for some ACSR cables. Designation according to standard UNE-EN 50 182 [49] (the Spanish standard equivalent to IEC 61089 [44]).

Voltage (kV)	**147-AL1/34-ST1A** [a]	**242-AL1/39-ST1A**	**402-AL1/52-ST1A**
	Power limit (cos φ = 0.8) (MVA)		
45	26.95	36.11	50.38
66	39.53	52.96	73.89
132	79.05	105.91	147.79
220	Not used	Not used	246.31
–	147-AL1/34-ST1A	242-AL1/39-ST1A	402-AL1/52-ST1A
–	Resistance at 85 °C		
r_{CL} (Ω/km)	0.2483	0.1195	0.0719

[a] According to UNE—EN 50 182 [49] the first number indicates the area (in mm^2) of aluminium and the second one the area (in mm^2) of steel.

Regarding the substation transformer, for the chosen power of 54 MW, the nameplate power should be around 60 MVA. For a power transformer of this nominal power, the short circuit impedance must be upper than 11% according to what is establish in the standard IEC 60076-5 [50].

Table 4 shows a summary of the parameters included in the simulations to model the WF and the rest of the electrical equipment necessary for the connection to the PCC.

Table 4. Characteristics of the new infrastructure elements used in the simulation of the entire WF.

Element	Name	Value	Unit	Comment
Wind Farm	Power	54	MW	18 × 3 MW
	Composition	3 circuits 6 WTG per circuit	–	–
Substation transformer	Nominal Power	60	MVA	–
	Po_{ST}	40	kW	Manufacturer data
	Ucc	11.00	%	According to standard IEC 60076 [50]
–	x/r	35	–	IEEE Transformers Committee recommendations [51]
PCC Voltage	V_{GRID}	132	kV	Typical
Evacuation line	Length (L)	15	km	–
	Material	147-AL1/34-ST1A	–	Designation according to standard UNE-EN 50 182 (Spanish standard equivalent to IEC 61089). See Table 3
	r_{CL} per km	3.7251	Ω/km	Value for the cable selected. Source [49]

3.2.4. Simulation Results and Sensitivity Analysis

First of all the losses of a circuit made up of 6 WTGs up to the BUS_{ST} were calculated The simulation was done by applying Equation (33) to only one circuit, so that:

$$El_{n_j} = T \sum_{s=0}^{s_{cut-out}} PN_{n_j}(s)\, f(s) \Delta s \tag{45}$$

And therefore:

$$El_{n_j}(\%) = \frac{El_{n_j}}{6 \times Eg} \times 100 \tag{46}$$

The results of the simulation are shown in Figure 10. Unlike the results for one WTG, now the losses calculated at rated power cannot be considered as a minimum because for several values of the Weibull parameters the actual losses go below it.

In the simulation represented in Figure 10, the size of the collector system cable was saaumed to be as indicated in Table 2. Generally the dimensioning of the collector system will depend on the characteristics of the WF as well as on the requirements of drop voltage and ampacity, so that it is important to analyse the sensitivity of the losses respect to the cable size. With this objective the simulation of the sensitivity of the ratio of the actual losses to the losses at rated power with the wind resource and the cable size was carried out The variation of the wind resource was implemented by maintaining fixed the shape parameter k = 2 (Rayleigh distribution) and modifying the scale parameter (λ) and the variation of the cable size modifying the value of the resistance r_C. The results are presented in Figure 11. As it can be noted, generally, except in the case of both high wind resource (high scale parameter) and high cable resistance the losses at rated power are an upper limit for the actual losses.

Figure 10. Electric losses of the energy generated for a circuit of six WTGs as a function of the Weibull parameters representative of the period considered.

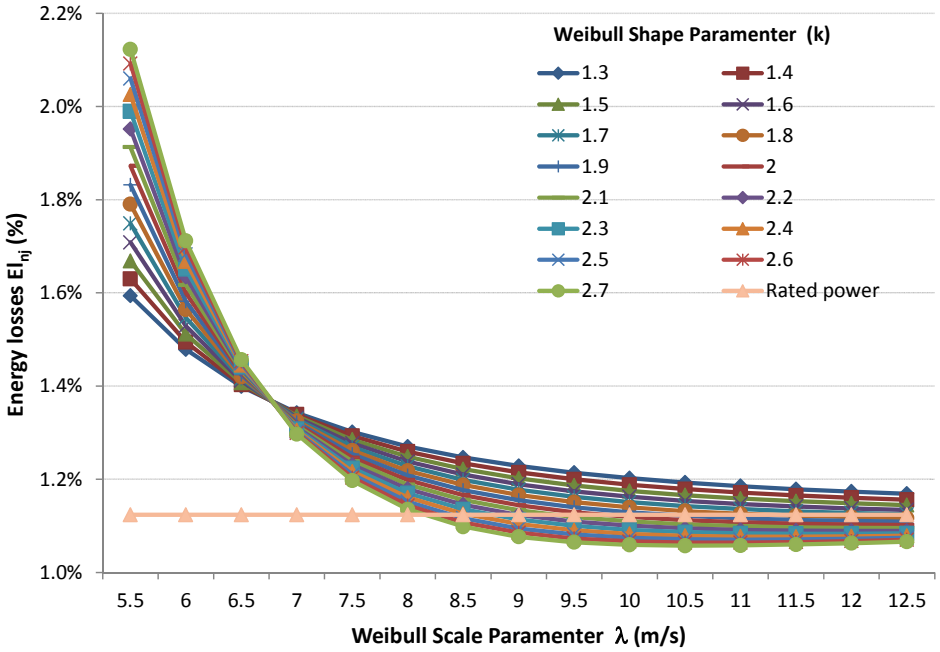

Figure 11. Sensitivity of the electric losses of the energy generated for a circuit of six WTGs with the value of the resistance of the collector system cable and with the scale Weibull parameter representative of the period considered considering the Weibull shape parameter equal to 2.

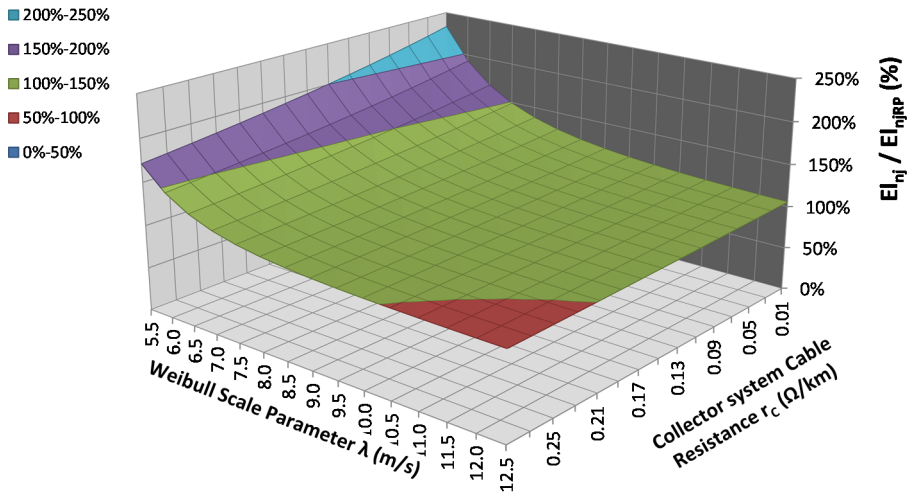

For the entire WF, considering Equation (43), the electricity losses as a percentage of the generation are:

$$El_{WF}(\%) = \frac{El_{WF}}{Eg_{WF}} \times 100 \tag{47}$$

The electricity losses at rated power are a particular case when the wind speed is equal or higher to s_{rated}, and can be obtained with the following expression:

$$El_{WF_{FP}}(\%) = 100 \times \frac{PN_{SET}}{PG_{WF}}\Big|_{s=s_{rated}} \tag{48}$$

The result of the simulation is illustrated in Figure 12. Unlike the results obtained for one WTG or a group, when the entire WF is considered, the actual losses are, practically in all the wind range, under the losses calculated when the WF operates at rated power which could be considered as a upper limit.

Figure 12. Electric losses of the energy generated for the WF as a function of the Weibull parameters representatives of the period considered.

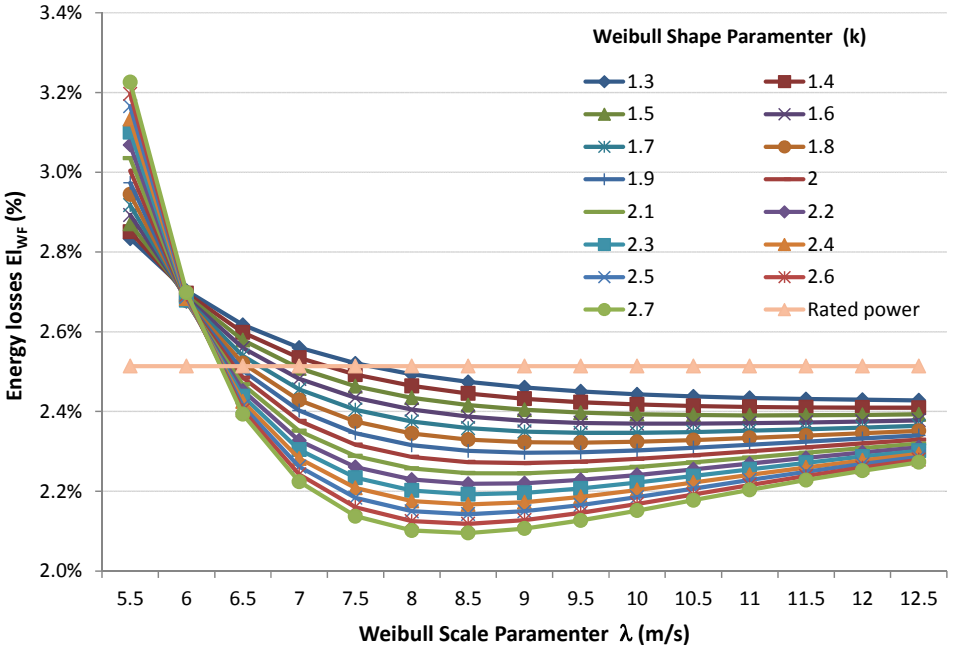

The length and the design of the evacuation line, as well as the PCC voltage level have a significant effect in the total losses, because by the line flows the total power and the losses are directly proportional to square of the active power flowing and are inversely proportional to the PCC voltage level.

With the aim of evaluating the effect the variation of these parameters on the electric losses, a sensitivity analysis was carried out with respect to them, by calculating the sensitivity of the ratio of the actual losses to the losses at rated power, with the wind resource and the type of conductor of the evacuation line. Once again, the variation of the wind resource was implemented by maintaining fixed the shape parameter k = 2 (Rayleigh distribution) and modifying the scale parameter (λ) and the variation of the conductor modifying the value of the resistance r_{CL}, in a range enough to cover all the types included in Table 3. Due to the effect of the PCC voltage magnitude in the losses, simulations were made for two different values widely used. The results are illustrated in Figure 13, where is shown how the actual losses for a particular infrastructure can be lower or higher than the losses at rated power, which is evidence that the latter should not be considered as a reference value in any case.

Figure 13. Sensitivity of the electric losses of the WF with the value of the resistance of the evacuation line cable and with the scale Weibull parameter representative of the period considered (Weibull shape parameter equal to 2) for two PCC voltage level. (**a**) 45 kV and (**b**) 132 kV.

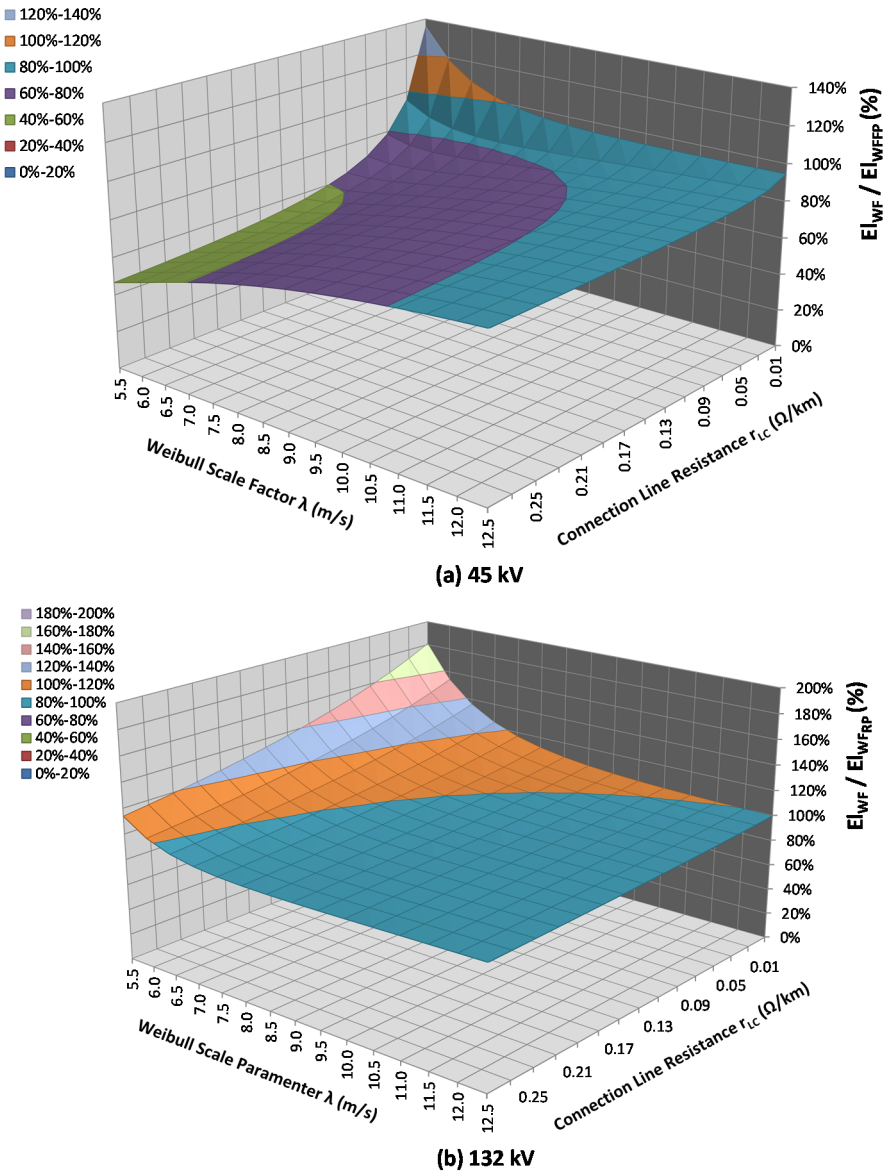

3.3. Comparative of the Behaviour of the Electric Losses

As can be noticed in Figures 6 and 12 there is a clear difference in the behaviour of the electric losses with respect of those calculated at rated power for each one of the both cases analysed: whereas for a single WTG the losses at rated power mean a minimum, for the entire WF the losses at rated power implies a maximum for almost all the range of the Weibull parameters except for periods with low wind resource (low scale parameter).

This distinct behaviour arises mainly from the different weight of the non-load losses (not depending on the wind resource) with respect to the total. For a single WTG and a circuit of several, due to the presence of the step-up transformers, the non-load losses represent a higher ratio than in the case of the entire WF because the addition of the load losses from the evacuation line and the substation transformer.

In case of a circuit of six WTG, the behaviour is similar to a single WTG except for periods with high wind resource, in which the load losses in the collector system increases (Figure 10).

3.4. Validity of the Proposed Method

To check the validity of the proposed method, it was applied to two real wind farms sited in different locations: Spain (25.2 MW with nine wind turbines of 1.8 MW and three of 3 MW and Argentina (51 MW with wind turbines of 3 MW). The method was applied for several periods during 2013 and 2014, with different wind conditions and in which the functioning of the wind farms were not affected by any unusual conditions (*i.e.*, big corrective maintenance). In all the cases the results obtained by the application of the simplified method proposed in this paper were in a gap of ±6% of real data for the electric losses.

4. Impact of the Losses in the Financial Value of the WF

The electric losses reduce the income resulting from selling the electricity generated by the WF. These incomes are the only source to repay the financing obtained to develop and build the WF. Although the reduction is not a very important percentage with respect to the income, the recurrence during the WF service life has an impact in the net value of the WF as an investment that must be considered.

The Net Present Value (NPV) is a classical way to state how much an investment is worth. It is defined as the sum of the present values of the individual cash flows updated to the construction year at a set up discount rate, reduced by the investment costs. It is calculated according to the following Equation [52]:

$$NPV = \sum_{z=1}^{n} \frac{CF_z}{(1+r)^z} - I \tag{49}$$

Where the yearly cash flows are calculated as it is detailed in Table 5.

Table 5. Cash flow calculation methods Self-elaboration.

	Cash Flow
+	Incomes from electricity remuneration
−	Operating expenses
=	Gross operating margin (EBITDA)
−	Depreciation
=	Earnings before interests and taxes (EBIT)
−	Financial expenses
=	Earnings before taxes
−	Taxes
=	Earnings after taxes
+	Depreciation
=	Yearly cash flow (CF_z)

As can be noticed in Equation (49), the variation of the NPV is linear with respect to the incomes and subsequently to the losses. As a practical example to establish the range of this variation, the effect in

the expected NPV was calculated for a WF with the characteristics detailed in Section 3.2.3., in function of the difference between the losses calculated following the method proposed in this article and the losses calculated at rated power. In the calculations were taken into account the assumptions included in the Table 6, which are all currently applicable to the WF studied.

Table 6. Assumptions for NPV calculation.

Breakdown	Name	Value	Unit	Comment
Prices	Wind Farm Construction	1,100	€/kW	Sources [13,30,53,54]
	Wind Farm O&M	20.00	€/MWh	Source [8,53]
	Land easements	3,000	€/(MW × year)	Includes assembly areas
	Insurance	0.50	% Incomes	All risk and Civil Liability. Typically calculated over incomes
	Administration	0.02	% Incomes	Typically calculated over incomes
	Yearly prices increase	2	%	Typically indexed to inflation. Estimate based on the trend in the inflation forecast [55,56]
Power purchase agreement	Initial PPA price	80.00	€/MWh	Estimated from [10]
	Yearly increase	2	%	Typically indexed to inflation. Estimate based on the trend in the inflation forecast [55,56]
Electricity generation	Gross capacity factor	30	%	–
	Wake losses	5	%	–
	Losses factor	1	%	Includes up to grid connection point
	WTG Mechanical Availability	97	%	WTG Mechanical availability is defined typically in a yearly period, as the percentage of time (year) in which the WTG is ready to roduce electricity Current market value. Source: WTG Manufacturers
Taxes	Profit taxes	30	%	–
	Income taxes	2	%	The final value depends on council and the incomes level. Mean value has been taken into consideration
Financial terms	Depreciation period	10	years	Typical

Figure 14 shows the reduction of the NPV, calculated for an estimated discount rate of 3% (value around the current inflation level in the euro zone), as a function of the ratio of the actual losses to the losses at rated power. In the example, the calculations give a reduction in the NPV around a 0.08% for every 5% of increase of the losses ratio, even reaching to a reduction close to 1.6% if the actual losses double the estimate at rated power.

With the aim to have an order of magnitude of this reduction, Figure 14 includes the loss of NPV in monetary terms for a WF with the characteristics of the Table 4. The important reduction, exceeding 2.3 M€ in case of double losses than estimated can be noticed.

Figure 14. Variation of the NPV with the energy losses.

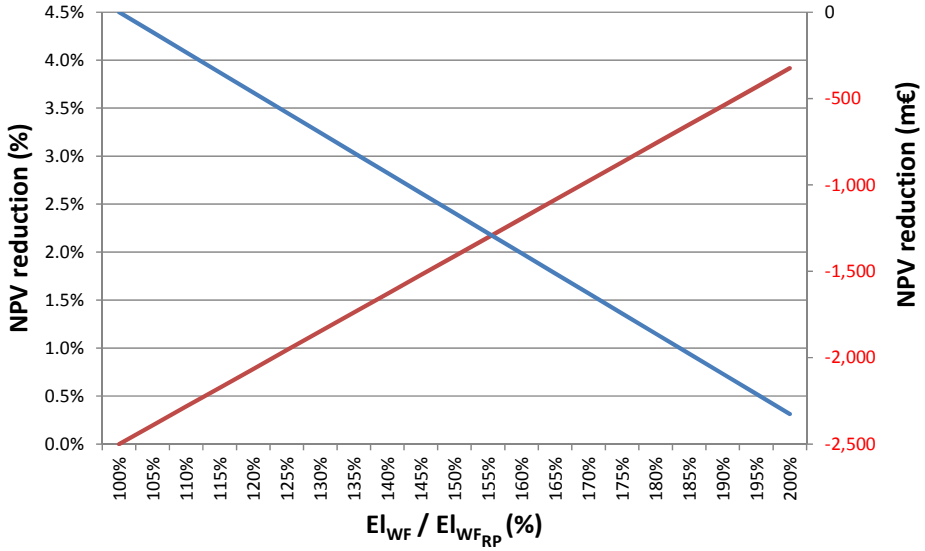

5. Conclusions

The electric losses calculated when all the WTGs in the WF operate at rated power cannot be used as a reference to define or guarantee the losses produced in the WF under actual operating conditions. Depending on the characteristics of the electrical infrastructures of the WF, as well as the real wind resource, the differences could be very important, even doubling or halving the expected value.

It is not possible to set a fixed value to define the expected losses. It is necessary to build a model of the WF, capable considering the actual wind conditions in the set period, to prove if the behaviour of the WF was according to the requirements. Besides, with this method it would be possible to detect, even in the short term, variations in the electric parameters considered in the model and it could be a complementary tool to prevent problems in the electrical infrastructure.

The method used for the analytical fit of the WTG power curve, together with the methodology for the simplified calculation of the actual electric losses established in Section 3.2.1., can be used as a simple tool to define *a priori*, in the design stage, the expected losses and to verify, considering the actual wind resource during, the correct behaviour of the WF. This methodology, with certain tolerances appropriate to the simplifications made, offers the possibility to do the verifications at any time and for any period of time.

The lack of definition produces an uncertainty, minor but perceptible, concerning the cash flows of the WF and therefore implies a relevant impact in its net value as investment.

Nomenclature

Weibull distribution	
$f(s)$	Probability density function for the wind speed Weibull distribution
λ	Scale parameter of the Weibull distribution (m/s)
k	Shape parameter of the Weibull distribution
$F(s)$	Cumulative distribution function for the wind speed Weibull distribution.
s	Wind speed (m/s)

Wind turbine and wind farm characteristics

BUS_{PCC}	Point of common coupling bus
BUS_{ST}	Bus of connection to all the collector system circuits with the evacuation line. Represents the wind farm substation.
BUS_{WTG}	Bus in which the wind turbine is connected to the collector system.
n_C	Number of electric circuits in the wind farm
n_{WF}	Number of wind turbines in the wind farm
PCC	Point of common coupling
r_C	Resistance of the interconnection cable to the collector system
r_{CL}	Resistance of the interconnection line
r_{ST}	Resistance representative of load active power losses in the substation transformer
r_T	Resistance representative of load active power losses in the internal wind turbine step-up transformer
V_{PCC}	Voltage magnitude in the point of common coupling
V_{GRID}	Voltage magnitude of the collector system
WF	Wind Farm
WTG	Wind turbine generator

Power flow analysis

b_{pij}	Parallel susceptance between buses i and j
B_{ij}	Serial susceptance between buses i and j
G_{ij}	Serial conductance between buses i and j
P_{ij}	Active power flow from bus i to bus j
Q_{ij}	Reactive power flow from bus i to bus j
V_i	Voltage magnitude in the bus i.
$\overline{Y_{ij}}$	Admittance between buses i and j.
θ_{ij}	Difference between the voltage angles in buses i and j.

Financial

NPV	Net present value
CF_z	Project cash flow in the year z
z	Ordinal indicating the number of years the PV system has been in service.
I	Investment value
r	Discount rate for NPV calculation

Wind turbine generator power curve

a, b, c	Coefficients of the polynom power curve adjust
P_{WTG}	Power output of the wind turbine
P_{WTGT}	Power output of the wind turbine minus the electric losses in the step-up transformer
P_{rated}	Rated power of the wind turbine
s_{cut-in}	Minimum wind speed at which the wind turbine will generate usable power
$s_{cut-out}$	Wind speed at which wind turbine cease power generation and shut down
s_{rated}	Minimum wind speed at which the wind turbine produces the rated power

Energy and power flow

CF	Capacity factor
Eg	Electricity generated by a wind turbine in the period T
Eg_{WF}	Electricity generated by the entire wind farm
El	Electricity losses in the period T

El_{RP}	Electricity losses when the wind turbine operates at rated power
El_{n_j}	Energy losses in the circuit n_j
$El_{nj_{RP}}$	Energy losses in the circuit n_j when all the wind turbines in the circuit operate at rated power
El_{WF}	Energy losses for the entire wind farm
$El_{WF_{RP}}$	Energy losses for the entire wind farm when all the wind turbines operate at rated power
PG_{WF}	Active power generated
Pl	Active power losses
Pl_C	Active power losses in the collector system cable
Pl_o	Active power losses when the wind turbine is not generating power
Pl_{rated}	Active power losses when the wind turbine operates at rated power
Pl_T	Load active power losses in the internal wind turbine step-up transformer
Pl_{WF}	Active power losses for the entire wind farm
PN_{ANY}	Net active power injected in the bus indicated (any)
Po_{ST}	No-load active power losses in the substation transformer
Po_T	No-load active power losses in the internal wind turbine step-up transformer
T	Period of time for energy calculations

Appendix A: Solution for the Integral

The integral to be solved is:

$$\int_{s_1}^{s_2} \sum_{i=0}^{n} a_i s^i f(s) ds = \int_{s_1}^{s_2} \sum_{i=0}^{n} a_i s^i \frac{k}{\lambda} \left(\frac{s}{\lambda}\right)^{k-1} e^{-\left(\frac{s}{\lambda}\right)^k} ds = \frac{k}{\lambda^k} \sum_{i=0}^{n} a_i \int_{s_1}^{s_2} s^{(k-1+i)} e^{-\left(\frac{s}{\lambda}\right)^k} ds \quad \text{(A1)}$$

The incomplete gamma function γ is defined as:

$$\int_u^v x^{(\alpha-1)} e^{-x} dx = \int_0^v x^{(\alpha-1)} e^{-x} dx - \int_0^u x^{(\alpha-1)} e^{-x} dx = \gamma(\alpha, v) - \gamma(\alpha, u) \quad \text{(A2)}$$

Doing the following change of variable:

$$x = \left(\frac{s}{\lambda}\right)^k ; s = \lambda x^{\frac{1}{k}}; \; dx = \frac{k}{\lambda}\left(\frac{s}{\lambda}\right)^{k-1} ds = \frac{k}{\lambda}\left(x^{\frac{1}{k}}\right)^{k-1} ds = \frac{k}{\lambda} x^{\left(\frac{k-1}{k}\right)}; \; ds = \frac{\lambda}{\mathrm{k}} \frac{dx}{x^{\left(\frac{k-1}{k}\right)}} \quad \text{(A3)}$$

The integral is given now by:

$$\frac{k}{\lambda^k} \sum_{i=0}^{n} a_i \int_{s_1}^{s_2} s^{(k-1+i)} e^{-\left(\frac{s}{\lambda}\right)^k} ds = \frac{k}{\lambda^k} \sum_{i=0}^{n} a_i \int_{\left(\frac{s_1}{\lambda}\right)^k}^{\left(\frac{s_2}{\lambda}\right)^k} \left(\lambda x^{\frac{1}{k}}\right)^{(k-1+i)} e^{-x} \frac{\lambda}{k} \frac{dx}{x^{\left(\frac{k-1}{k}\right)}} = \sum_{i=0}^{n} a_i \lambda^i \int_{\left(\frac{s_1}{\lambda}\right)^k}^{\left(\frac{s_2}{\lambda}\right)^k} x^{\frac{i}{k}} e^{-x} dx \quad \text{(A4)}$$

Identifying the parameter α of the incomplete gamma function:

$$\alpha - 1 = \frac{i}{k}; \alpha = \frac{i}{k} + 1 \quad \text{(A5)}$$

Finally, the solution of the integral is:

$$\int_{s_1}^{s_2} \sum_{i=0}^{n} a_i\, s^i\, f(s)ds = \sum_{i=0}^{n} a_i\, \lambda^i \left\{ \gamma\left[\left(\frac{i}{k}+1\right), \left(\frac{s_2}{\lambda}\right)^k\right] - \gamma\left[\left(\frac{i}{k}+1\right), \left(\frac{s_1}{\lambda}\right)^k\right]\right\} \quad \text{(A6)}$$

Author Contributions

All the authors equally contributed during the writing and the critical revision of the paper, according to the reviewers' comments.

Conflicts of Interest

The authors declare no conflict of interest.

References

1. Díaz-Dorado, E.; Carrillo, C.; Cidrás, J.; Albo, E. Estimation of Energy Losses in a Wind Park. In Proceedings of the 9th International Conference Electrical Power Quality and Utilisation, Barcelona, Spain, 9–11 October 2007.
2. González, J.S.; Gonzalez Rodriguez, A.G.; Mora, J.C.; Santos, J.R.; Payan, M.B. Optimization of wind farm turbines layout using an evolutive algorithm. *Renew. Energy* **2010**, *35*, 1671–1681.
3. Inaba, N.; Takahashi, R.; Tamura, J.; Kimura, M.; Komura, A.; Takeda, K. A Consideration on Loss Characteristics and Annual Capacity Factor of Offshore Wind Farm. In Proceedings of the 2012 XXth International Conference on Electrical Machines (ICEM), Marseille, France, 2–5 September 2012; IEEE: New York, NY, USA, 2012; pp. 2022–2027.
4. Takahashi, R.; Ichita, H.; Tamura, J.; Kimura, M.; Ichinose, M.; Futami, M.; Ide, K. Efficiency Calculation of Wind Turbine Generation System with Doubly-Fed Induction Generator. In Proceedings of the 2012 XXth International Conference on Electrical Machines (ICEM), Rome, Italy, 6–8 September 2010; IEEE: New York, NY, USA, 2010; pp. 1–4.
5. Camm, E.H.; Behnke, M.R.; Bolado, O.; Bollen, M.; Bradt, M.; Brooks, C.; Dilling, W.; Edds, M.; Hejdak, W.J.; Houseman, D.; *et al*. Wind Power Plant Collector System Design Considerations: IEEE PES Wind Plant Collector System Design Working Group. In Proceedings of the 2009. PES '09. IEEE Power & Energy Society General Meeting, Calgary, AB, Canada, 26–30 July 2009; IEEE: New York, NY, USA, 2010; pp. 1–7.
6. Camm, E.H.; Behnke, M.R.; Bolado, O.; Bollen, M.; Bradt, M.; Brooks, C.; Dilling, W.; Edds, M.; Hejdak, W.J.; Houseman, D.; *et al*. Wind Power Plant Substation and Collector System Redundancy, Reliability, and Economics. In Proceedings of the 2009. PES '09. IEEE Power & Energy Society General Meeting ; Power & Energy Society General Meeting, Calgary, AB, Canada, 26–30 July 2009; IEEE: New York, NY, USA, 2010; pp. 1–6.
7. Steimer, P.K.; Apeldoorn, O. Medium voltage power conversion technology for efficient windpark power collection grids. In Proceedings of the 2010 2nd IEEE International Symposium on Power Electronics for Distributed Generation Systems (PEDG), Hefei, China, 16–18 June 2010; IEEE: New York, NY, USA, 2010; pp. 12–18.
8. Blanco, M.I. The economics of wind energy. *Renew. Sustain. Energy Rev.* **2009**, *13*, 1372–1382.

9. The European Wind Energy Association. Wind in Power 2013. Available online: http://www.ewea.org/fileadmin/files/library/publications/statistics/EWEA_Annual_Statistics_2013.pdf (accessed on 21 September 2014).
10. Asociación Empresarial Eólica. *Eólica 2014*; Asociación Empresarial Eólica: Madrid, Spain, 2014. (In Spanish)
11. U.S. Department of Energy. *Wind Technologies Market Report 2012*; U.S. Department of Energy: Oak Ridge, TN, USA, 2013.
12. Kalamova, M.; Kaminker, C.; Johnstone, N. *Source of Finance, Investment Policies and Plant Entry in the Renewable Energy Sector*; OECD Publishing: Paris, France, 2011.
13. U.S. Department of Energy. *Wind Technologies Market Report 2012*; Lawrence Berkeley National Laboratory: Berkeley, CA, USA, 2013.
14. Department of Energy Republic of South Africa Renewable Energy. Independent Power Producer Procurement Programme. Available online: http://www.ipprenewables.co.za/ (accessed on 25 June 2014).
15. McGovern, M. Analysis—Uruguay, the next big South American market. In *Wind Power Monthly*; Haymarket Media Group Ltd.: London, UK, 2013.
16. Carrillo, C.; Cidrás, J.; Díaz-Dorado, E.; Obando-Montaño, A.F. An Approach to Determine the Weibull Parameters for Wind Energy Analysis: The Case of Galicia (Spain). *Energies* **2014**, *7*, 2676–2700.
17. Villanueva, D.; Feijó, A.; Pazos, J.L. Multivariate Weibull distribution for wind speed and wind power behavior assessment. *Resources* **2013**, *2*, 370–384.
18. Amenedo Rodríguez, J.L.; Burgos Díaz, J.C.; Arnalte Gómez, S. *Sistemas Eólicos de Producción de Energía Eléctrica*; Rueda: Madrid, Spain, 2003; p. 439. (In Spanish)
19. Carta González, J.A.; Calero Pérez, R.; Colmenar Santos, A.; Castro Gil, M.-A. *Centrales de Energías Renovables: Generación Eléctrica con Energías Renovables*; Pearson Educación, S.A.: Madrid, Spain, 2009; p. 703. (In Spanish)
20. Margaris, I.D.; Hansen, A.D.; Sorensen, P.; Hatziargyriou, N.D. Illustration of modern wind turbine ancillary services. *Energies* **2010**, *3*, 1290–1302.
21. Gómez Expósito, A.; Abur, A.; Alvarado, F.L.; Alvarez Bel, C.; Pérez Arriaga, J.I.; Rivier Abad, M. Flujo de cargas. In *Análisis y Operación de Sistemas de Energía Eléctrica*; McGraw-Hill Interamericana de España: Madrid, Spain, 2002; p. 769. (In Spanish)
22. Carrillo, C.; Obando Montaño, A.F.; Cidrás, J.; Diaz-Dorado, E. Review of power curve modelling for wind turbines. *Renew. Sustain. Energy Rev.* **2013**, *21*, 572–581.
23. Kusiak, A.; Zheng, H.; Song, Z. On-line monitoring of power curves. *Renew. Energy* **2009**, *34*, 1487–1493.
24. Lydia, M.; Kumar, S.S.; Selvakumar, A.I.; Prem Kumar, G.E. A comprehensive review on wind turbine power curve modeling techniques. *Renew. Sustain. Energy Rev.* **2014**, *30*, 452–460.
25. Vestas Vestas. Available online: http://www.vestas.com (accessed on 25 May 2014).
26. Siemens Wind Power. Available online: http://www.energy.siemens.com/hq/en/renewable-energy/wind-power/ (accessed on 2 June 2014).
27. Alstom Wind Power. Available online: http://www.alstom.com/power/renewables/wind/ (accessed on 25 June 2014).

28. Gamesa Corporation Gamesa. Available online: http://www.gamesacorp.com/en/ (accessed on 25 June 2014).
29. Prysmian Group. *Medium Voltage Cables Catalogue*; Prysmian Group: Milan, Italy, 2013.
30. Serrano González, J.; Burgos Payán, M.; Santos, J.M.R.; González-Longatt, F. A review and recent developments in the optimal wind-turbine micro-siting problem. *Renew. Sustain. Energy Rev.* **2014**, *30*, 133–144.
31. Shamsoddin, S.; Porté-Agel, F. Large eddy simulation of vertical axis wind turbine wakes. *Energies* **2014**, *7*, 890–912.
32. Son, E.; Lee, S.; Hwang, B.; Lee, S. Characteristics of turbine spacing in a wind farm using an optimal design process. *Renew. Energy* **2014**, *65*, 245–249.
33. Turner, S.D.O.; Romero, D.A.; Zhang, P.Y.; Amon, C.H.; Chan, T.C.Y. A new mathematical programming approach to optimize wind farm layouts. *Renew. Energy* **2014**, *63*, 674–680.
34. González-Longatt, F.; Wall, P.; Terzija, V. Wake effect in wind farm performance: Steady-state and dynamic behavior. *Renew. Energy* **2012**, *39*, 329–338.
35. Hasager, C.B.; Rasmussen, L.; Peña, A.; Jensen, L.E.; Réthoré, P.-E. Wind farm wake: the horns rev photo case. *Energies* **2013**, *6*, 696–716.
36. Porté-Agel, F.; Wu, Y.-T.; Chen, C.-H. A numerical study of the effects of wind direction on turbine wakes and power losses in a large wind farm. *Energies* **2013**, *6*, 5297–5313.
37. ABB Super-slim Switchgear for Wind Turbines. Available online: http://www.abb.com/cawp/seitp202/6bca779c32011d61c125770b003f7ee0.aspx (accessed on 25 June 2014).
38. Ormazabal Gas-insulated switchgear for secondary distribution systems. Available online: http://www.ormazabal.com/es/tu-negocio/productos/cgm3–36-kv-iec-630–21-ka?refer=1300 (accessed on 20 June 2014).
39. Siemens Gas-insulated Switchgear for Secondary Distribution Systems. Available online: http://w3.siemens.com/powerdistribution/global/EN/mv/medium-voltage-switchgear/gis-secondary-distribution-systems/Pages/gas-insulated-switchgear-for-secondary-distribution-systems.aspx (accessed on 28 May 2014).
40. International Electrotechnical Commission. *Wind Turbines. Part 1: Design Requirements*; International Electrotechnical Commissio: Geneva, Switzerland, 2005; Volume IEC 61400-1.
41. Mathworks. *Matlab*, R2012a; Mathworks: Natick, MA, USA.
42. Dutta, S.; Overbye, T.J. A Clustering Based Wind Farm Collector System Cable Layout Design. In Proceedings of the Power and Energy Conference, Urbana, IL, USA, 25–26 February 2011; IEEE: New York, NY, USA, 2011; pp. 1–6.
43. Feltes, J.W.; Fernandes, B.S.; Keung, P.K. Case Studies of Wind Park Modeling. In Proceedings of the Power and Energy Society General Meeting, Detroit, MI, USA, 24–29 July 2011; pp. 1–7.
44. International Electrotechnical Commission. *Round Wire Concentric Lay Overhead Electrical Stranded Conductors*; International Electrotechnical Commissio: Geneve, 1991; Volume IEC 614089.
45. General Electric Industrial Transformers—Power. Available online: http://www.geindustrial.com/products/transformers/power-0 (accessed on 25 June 2014).
46. Siemens Power Transformers. Available online: http://www.energy.siemens.com/hq/en/power-transmission/transformers/power-transformers/medium-power-transformers.htm (accessed on 25 June 2014).

47. General Cable Technologies Corporation General Cable Cables. Available online: http://es.generalcable.com/dgeneralcable/GeneralCable/ (accessed on 25 June 2014).
48. Southwire Southwire Product Catalogue. Available online: http://www.southwire.com/products/ProductCatalog.htm (accessed on 30 May 2014).
49. Spanish Association for Standardisation and Certification. *Conductores Para Líneas Eléctricas. Conductores de Alambres Redondos Cableados en Capas Concéntricas*; AENOR: Madrid, Spain, 2002; Volume UNE-EN 50182.
50. International Electrotechnical Commission. *Power Transformers. Part 5: Ability to Withstand Short Circuit*; International Electrotechnical Commissio: Geneve, Spain, 2000; Volume IEC 60076–5.
51. IEEE Transformers Committee, Performance Characteristics Subcommittee. x/r Discussion. In 2003. Available online: http://grouper.ieee.org/groups/transformers/subcommittees/performance/WG_C57_12_00/XoverRdiscussion.pdf (accessed on 25 June 2014).
52. Pérez Gorostegui, E. *Introducción a la Economía de la Empresa*; Editorial Centro de Estudios Ramón Areces: Madrid, Spain, 2007. (In Spanish)
53. International Renewable Energy Agency. *Renewable Energy Technologies: Cost Analysis Series. Volume 1: Power Sector. Issue 5/5. Wind Power*; International Renewable Energy Agency (IRENA): Abu Dhabi, United Arab Emirates, 2012.
54. IDAE Ministerio de Industria Turismo y Comercio. *Plan de Energías Renovables 2011–2020*; Gobierno de España: Madrid, Spain, 2011. (In Spanish)
55. European Commission Economic Financial Affairs Economic Forecasts. Available online: http://ec.europa.eu/economy_finance/eu/forecasts/index_en.htm (accessed on 25 June 2014).
56. PWC Economic Projections. Available online: http://www.pwc.com/gx/en/issues/economy/global-economy-watch/projections/june-2014.jhtml (accessed on 15 June 2014).